This research was supported by the NASA Langley Research Center under contract No. NAG-1526, 10/11/84-10/10/85.

CLOSURE MEASUREMENTS ON SHORT FATIGUE CRACKS

by

J. J. Lee and W. N. Sharpe, Jr.
The Department of Mechanical Engineering
The Johns Hopkins University
Baltimore, MD 21218

Presented at the ASTM International Symposium on Fatigue Crack Closure, Charleston, SC, May 1986. Accepted for publication in ASTM STP.

ABSTRACT

Single-edged notched specimens, 2.3 mm thick, of 2024-T3 aluminum were cyclicly loaded at R-ratios of 0.5, 0.0, -1.0, and -2.0. The notch roots were periodically inspected with an optical microscope in order to locate the initiation of very short cracks. Acetate replicas were also taken. The loads were selected to produce fatigue lives of 500,000 cycles or less. The specimens and the load schedules were part of an AGARD-sponsored, round-robin test program designed to study the growth of short cracks.

As an addition to the AGARD program, crack opening displacements were measured at single positions across cracks as short as 0.035 mm and as long as the full thickness of the specimen. Two small reflective indentations were placed across the short crack and illuminated with a 35-milliwatt He-Ne laser. This formed interference fringe patterns that could be monitored to measure the relative displacement between the two indentations. Fringe motion was monitored with a minicomputer-controlled optical scanning system to produce real-time crack opening displacements.

The load-displacement record is stored and analyzed after the test to determine the opening load. This is accomplished by fitting a straight line to the data points in the linear region of the plot after the crack is completely open. The fitted line is subtracted from the plot, and when the deviation of this reduced data from zero exceed a preset value, the opening load is established. One also obtains the compliance of the fully opened crack from the analysis of the data.

The opening load ratios for the short cracks are somewhat smaller than those for long cracks at positive R-ratios, but are considerably smaller for negative R-ratios. The measured compliances of the very short cracks increase linearly with increasing surface crack length and agree quite well with the predictions of linear elastic fracture mechanics.

INTRODUCTION

It is generally recognized that short cracks tend to propagate faster than long cracks when the comparison is based on the stress intensity factor. One possible mechanism to explain this behavior is the phenomenon of crack closure. Plasticity induced closure results from the wake of residual compressive stresses left behind the growing fatigue crack. The length of this wake is obviously much smaller for a short crack, so closure would be expected to have less of an effect. This means that the short crack would experience a larger effective stress intensity factor range (ΔK_{eff}) than a long crack subjected to the same nominal ΔK and would therefore grow at a faster rate. In order to evaluate this hypothesis, it is necessary to be able to determine the loads at which a short crack becomes fully open, i.e., the closure loads.

Closure loads are normally determined from records of load versus displacement. When the crack becomes fully open, the upper portion of this record becomes linear corresponding to the compliance of the cracked specimen. The load at which this occurs is the closure load. Procedures for establishing this value are not yet standardized. The usual displacement measuring techniques used for long cracks, such as clip gages or foil gages on the back of the specimen, are too insensitive for use on short cracks. Morris et al [1] have used scanning electron microscopy for specimens loaded in the SEM chamber to measure the opening displacement. Davidson [2] has used stereo microscopy to measure the displacements near the tips of cracks. Both of these techniques have high resolution but are somewhat tedious.

In this study, crack opening displacements were measured for short surface cracks and for full-width surface cracks initiating at the roots of notches in aluminum specimens. The cracks were measured using an Interferometric Strain/ Displacement Gage (ISDG). This minicomputer-controlled measurement system has a resolution of 0.02 micrometer over gage lengths as short as a few tens of micrometers and enables real-time displacement measurement with storage of the data for post-processing to establish the closure load. Closure loads and compliances were determined for various R-ratios and gross stress levels.

SPECIMENS AND LOADING CONDITIONS

The specimens and loading conditions were provided by NASA-Langley as part of an AGARD-sponsored, round-robin test program to study the growth of short cracks. Participants were required to measure the initiation and growth of short cracks with acetate replicas. The round-robin procedures were followed explicitly for the data reported here; in addition, crack opening displacements were measured at single positions across selected short cracks to investigate their closure.

The test specimens were made from a 2024-T3 aluminum sheet, 2.3 mm thick, with a yield stress of 359 MPa. Figure 1 shows the shape of the specimen, which had a stress concentration factor of 3.17 [3]. Each specimen was chemically polished to remove the residual stresses which are induced by the rolling and machining processes. The specimens were prepared at NASA, thus guaranteeing uniformity for the round-robin test program. Twenty-four specimens were tested under constant amplitude loading at load ratios of R = 0.5, 0.0, -1.0, and -2.0. At each load ratio, three different stress levels (Smax) were applied, providing a total of twelve different loading conditions:

Smax = 225 MPa, 205 MPa, and 195 MPa for R = 0.5;
Smax = 145 MPa, 120 MPa, and 110 MPa for R = 0.0;
Smax = 105 MPa, 80 MPa, and 70 MPa for R = -1.0;
Smax = 75 MPa, 60 MPa, and 50 MPa for R = -2.0.

Prior to testing in an electrohydraulic test machine, the special fixtures gripping the specimen were carefully aligned to prevent rotational and lateral bending. A strain-gaged specimen was used to adjust the grips to within the tolerances specified by the test program. Anti-buckling guide plates were loosely bolted on either side of the specimen to prevent buckling under compressive loading.

The specimen was cycled at 20 Hz with a sinusoidal wave. Surface crack growth was monitored using the acetate replica technique at intervals ranging from 2,000 cycles at the highest stress level to 10,000 cycles for the lowest stress level at each R-ratio. An optical microscope was used to examine the replicas and measure the surface crack lengths.

Twelve specimens were cycled under the twelve loading conditions described previously until a crack was grown through the thickness, but not along the sides, of each specimen. These tests provided the necessary crack growth data and permitted closure measurements on longer cracks. The other twelve specimens were also cycled under each of the loading conditions, but only until a very short crack appeared in each of them. These specimens were then used for measuring the closure behavior of extremely short cracks.

CRACK OPENING DISPLACEMENT MEASUREMENT PROCEDURES

The Interferometric Strain/Displacement Gage (ISDG) has a very small gage length and can measure relative displacement with a resolution of approximately 0.02 micrometer. Only a brief discussion will be included here; for more details, see reference 4.

Two small indentations are pressed into the specimen surface across a crack using the pyramid-shaped diamond tip of a Vicker's micro-hardness tester. When these two indentations are illuminated with a laser, the reflections from the four sides form interference patterns in space. As the indentations move away from each other, the fringe patterns also move, and this motion is easily associated with the relative displacement, δd:

$$\delta = \frac{\Delta m_u + \Delta m_l}{2} \cdot \frac{\lambda}{\sin \alpha_o}$$

where λ is the wavelength of the laser and α_o is the angle between the incident laser beam and the reflected fringe pattern. Δm_u and Δm_l are the relative fringe motions of the two patterns in the plane containing the axis of measurement.
is equal to 632.8 nm for the He-Ne laser used in this experiment, while α_o is approximately 42°. Thus, the calibration factor,

$$\frac{\lambda}{\sin \alpha_o}$$

is about 1 μm.

Load versus crack opening displacement was measured using the ISDG, and the closure stress was determined from the data. The two indentations, both measuring 7-10 μm, were placed at a distance of 20-50 μm across the short cracks. Photographs of a pair of indentations placed across a crack 100 micrometers long, before the specimen was broken apart, are shown in Figure 2.

Figure 3 shows a typical load-displacement plot. The closure load (or the opening load), Pop, can be determined with reasonable accuracy by a reduced displacement method. A least-square line is fitted to the upper linear portion of the crack opening displacement curve. In the linear portion, it is assumed that the crack is fully opened. The reduced data are

obtained by subtracting values of the fitted line from the original data. Then the closure load is defined at the point where the reduced displacement becomes zero. It is difficult to pick the point where the reduced displacement is exactly equal to zero because the original data are not perfectly linear. The closure load can be determined at the point where the deviation of the reduced data becomes 10% of the maximum difference shown in Figure 3. This procedure is an arbitrary selection, but at least it is consistent from test to test.

RESULTS

Crack opening displacement (COD) was measured using the ISDG technique. Typical plots of load versus COD are shown in Figure 4 for R = -2.0 for surface cracks at the notch bore.

Figure 4 shows the COD curves for the surface cracks with lengths of 0.035 mm, 0.10 mm, and 0.17 mm which originated at the center of the notch bore and grew into semi-elliptical shapes. The maximum cyclic loads were 75 MPa in gross stress, 50 MPa, and 60 MPa, respectively. As shown in this plot, the crack is closed in the compressive load region and behaves as an elastic material until the crack begins to open. The elastic slope in the compressive load region was within 10% agreement with the modulus of this material (73,100 MPa) -- implying that the ISDG is certainly capable of measuring displacement with reasonable accuracy.

For the curve of the 0.035-mm crack, the measured COD was very small (0.16 micrometers at the maximum load), and the transition of the slope was hard to see on this large-scale plot. On an enlarged scale, it can be seen clearly. The slope transition for the 0.17-mm crack occurs at a point below zero, which indicates that the crack is fully opened at a compressive load. The compliance values calculated from this plot were 0.15×10^{-4} μm/Nt, 0.53×10^{-4} μm/Nt, and 1.09×10^{-4} μm/Nt respectively for these crack lengths.

The resulting crack compliances and closure load ratios for the short surface cracks and through-thickness cracks tested in this study are listed in Table I. Average crack depths for the through-thickness cracks were computed from the lengths at the center and the two quarter-points.

TABLE I.
Crack Compliances and Opening Load Ratios

Stress Ratio	Maximum Stress(MPa)	Crack Size 2a(mm)	Crack Size depth(mm)	Crack Shape	Compliance (μm/Nt)	Pop/ Pmax
0.5	225	0.54	0.42	C	1.59 E-4	0.34
	225	2.30	1.31	T	14.0 E-4	0.29
	205	0.18	-	S	1.3 E-4	0.32
	205	0.54	0.48	C	4.58 E-4	0.38
	195	0.40	0.18	S	2.17 E-4	0.39
0.0	145	2.30	1.1	T	15.0 E-4	0.33
	145	0.245	0.12	S	1.34 E-4	0.32
	120	2.30	2.69	T	31.2 E-4	0.21
	110	2.30	1.65	T	24.5 E-4	0.30
	110	0.414	0.38	C	4.21 E-4	0.34
-1.0	105	2.30	-	T	10.8 E-4	0.0
	105	0.19	-	S	0.9 E-4	0.0
	80	2.30	1.26	T	17.7 E-4	0.12
	80	0.05	-	S	0.46 E-4	0.12
	70	2.30	1.30	T	17.9 E-4	0.0
	70	0.2	-	S	0.91 E-4	0.18
-2.0	75	2.30	1.35	T	20.1 E-4	-0.18
	75	0.035	-	S	0.15 E-4	0.0
	60	2.30	0.88	T	10.4 E-4	-0.12
	60	0.17	-	S	1.09 E-4	-0.38
	50	2.30	1.23	T	16.8 E-4	-0.13
	50	0.10	0.04	S	0.53 E-4	0.0

S : surface crack in center
C : corner crack
T : through-thickness crack

Some of the crack depths could not be measured because the cracks could not be located on the fracture surface.

Surface cracks were found to be semi-elliptical in shape and corner cracks were quarter-elliptical. The measured crack depths were shown to be a constant ratio, approximately 0.9, to the semi-surface crack length for most cases. Thus the crack lengths may be compared simply with the surface lengths for this case where there is a constant ratio of surface length to depth.

Average crack depths computed from the lengths at the center and the two quarter-points were used instead of the surface crack lengths for through-thickness cracks (crack depths are listed in Table I).

Figure 5 is a comparison of compliance values for surface crack lengths of short surface cracks with lengths up to 0.5 mm. Each data point was tested at a different stress level, but no variation in compliance was noted. Also, no dependence of compliance upon R ratio was found for these short surface cracks. The compliance shows a linear relationship to the surface crack length, as shown by this plot. Similar results have been reported in other papers [1,5]. Morris and Buck [1] found a linear relationship between compliance and crack length and no variation of compliance with applied stress level for surface microcracks. James and Smith [5] also observed the linear relationship of compliance and crack length for small surface cracks. The compliance values measured for the very short surface cracks at the root of the notch agree very well with the predictions of Mattheck et al [6]. They computed the compliance of surface cracks in the presence of a stress gradient, and their prediction is plotted in Figure 5.

The variation of opening load levels with crack lengths is shown in Figure 6. Open symbols represent data from surface cracks whose lengths ranged from 0.035 mm to 0.5 mm; solid lines represent the opening stress ratios predicted for short cracks from Newman's calculated data [7]. Each data point was tested at a different stress level, as shown in Table I, but Newman's prediction was calculated for some specific stress level: $S_{max}/\tau_o = 0.25$ for R = 0.0; $S_{max}/\tau_o = 0.15$ for R = -1.0; $S_{max}/\tau_o = 0.15$ for R = -2.0. τ_o is the flow stress, corresponding to 427 MPa for Al 2024-T3, which is the average value of the yield stress (359 MPa) and the ultimate tensile stress (496 MPa).

Measured opening stress ratios for R = 0.5 were below the minimum cyclic stress. It is reasonable to define the opening stress as equivalent to the minimum cyclic stress for such a case. Newman's prediction for R = 0.5 shows that opening load ratio is the same as R-ratio. Most of the measured values in Figure 6 are smaller than the levels predicted for R = 0.0, -1.0, and -2.0. Predicted values show quick increases in the opening stress level while the crack is still very short (less than 0.08 mm) with a stabilization of opening stress for crack lengths greater than 0.1 mm. Measured data shows scattering in a wide band for lengths less than 0.2 mm. It can be observed from Figure 6 as a general trend that the opening stress levels increase as crack length increases, except for the case where R= -2.0.

Figure 7 shows the opening load ratio versus crack depth measured in the specimen width direction for through- thickness cracks. Also, opening stress ratio values predicted for a long crack from Newman's equation [8] are plotted to compare with measured data. Newman's equation for determining the crack opening stress for long cracks is expressed as follows.

$$\frac{S_{op}}{S_{max}} = A_o + A_1 R + A_2 R^2 + A_3 R^3 \quad \text{for } R \geq 0$$

and

$$\frac{S_{op}}{S_{max}} = A_o + A_1 R \quad \text{for } -1 \leq R < 0$$

where R is the stress ratio and the constants A_o, A_1, A_2, and A_3 are functions of the stress ratio, the stress level, and the constraint factor. Average opening stress ratios, calcutaed from the above equation over applied stress levels for R-ratios of 0.5, 0.0, and -1.0 are 0.55, 0.36, and 0.32, respectively; the extrapolated value for R = -2.0 is 0.30.

As shown in Figure 7, the opening stress levels for the through-thickness cracks tested in this study appears smaller in general than the values predicted by Newman for the long cracks. The difference between the opening stress levels is relatively small for R = 0.0 and substantially larger for negative R-ratios. This implies that when considering the growth behavior of short and long cracks, a greater difference between them should be expected for negative R-ratios than for positive R-ratios for the material tested in this study.

The measured opening stresses for the short surface or corner crack were smaller in general then those predicted for the long cracks. The same trend was observed for the through-thickness cracks whose average lengths were within the range of 0.8 - 2.7 mm in the direction of depth. This result indicates that even the through-thickness cracks with physically short lengths may have rates different from long cracks, as discussed in an earlier paper [9]. Similar behavior was observed in other experiments [10,11]. Leis and Forte [10] showed that even physically long cracks, i.e., as long as 2.5 mm in the aluminum alloys, also exhibit different growth behavior compared to longer-crack trends. Tanaka [11] observed the short-crack effect to lengths of 2 mm.

CONCLUSIONS

The Interferometric Strain/Displacement Gage technique is useful in measuring the crack opening displacement (COD) across cracks as short as 35 micrometers. Since it measures so close to the crack tip, the resulting load-COD data curves clearly show the change of slope in the crack compliance. This transition point indicates the crack opening or closure level.

The crack compliances, which were obtained from the upper linear portion of the COD curves, show linear relationships with the crack lengths for short surface cracks. They agree very well with the predictions of linear elastic fracture mechanics.

The opening stress ratios measured for the short surface cracks with lengths from 35 to 500 micrometers show a slight dependence upon crack length; but they also show lower values than those predicted for long cracks. The opening stress levels measured for the through-thickness cracks, those with depths between 0.8 and 2.7 mm, show a similar behavior.

The opening stress levels measured for R = 0.5 and 0.0 are approximately 1/3 of the maximum applied stress and agree well with the predicted values from the long cracks. The opening levels for R = -1.0 and -2.0 are zero or negative, and the differences between these values and the corresponding long-crack predictions are significant.

ACKNOWLEDGEMENTS

This work was supported by NASA grant NAG-1526 from Langley Research Center. The authors would like to thank Dr. Jim Newman and Mrs. Mary Swain for their technical guidance. John Cieslowski, an undergraduate student assisted with the experiments.

REFERENCES

(1) Morris, W. L.; and Buck, O.: Crack Closure Load Measurement for Microcracks Developed During the Fatigue of Al 2219-T851. Metallurgical Transactions A, vol. 8A, 1977, pp. 597-601.

(2) Hudak, S. J., Jr.: Small Crack Behavior and the Prediction of Fatigue Life. Transactions of ASME, vol. 103, 1981, pp. 26-35.

(3) Edwards, P. R.; and Newman, J. C., Jr.: AGARD Collaboration Effort on Short Cracks (Instructions to Participants). NASA Langley Research Center, 1984.

(4) Sharpe, W. N., Jr.: Application of the Interferometric Strain/Displacement Gage. Optical Engineering, vol. 21, no. 3, 1982, pp. 483-488.

(5) James, M. N.; and Smith, G. C.: Surface Microcrack Closure in Fatigue: A Comparison of Compliance and Crack Sectional Data. International Journal of Fracture, vol. 22, 1983, pp. R69-R75.

(6) Mattheck, C.; Morawietz, P.; and Munz, D.: Sress Intensity Factor at the Surface and at the Deepest Point of a Semi-elliptical Surface Crack in Plates Under Stress Gradients. International Journal of Fracture, vol. 23, 1983, pp. 201-212.

(7) Newman, J. C., Jr.; Swain, M. H.; and Phillips, E. P.: An Assessment of the Small-Crack Effect for 2024-T3 Aluminum Alloy.

(8) Newman, J. C., Jr.: A Crack Opening Stress Equation for Fatigue Crack Growth. International Journal of Fracture, vol. 24, 1984, pp. R131-R135.

(9) Lee, J. J.; and Sharpe, W. N., Jr.: Short Fatigue Cracks in Notched Aluminum Specimens. Presented at the Second International Workshop on Small Fatigue Cracks, January, 1986.

(10) Leis, B. N.; and Forte, T. P.: Fatigue Growth of Initially Physically Short Cracks in Notched Aluminum and Steel Plates. ASTM STP 743, 1981, pp. 100-124.

(11) Tanaka, K.: Short-Crack Fracture Mechanics in Fatigue Conditions. Current Research on Fatigue Cracks, pp. 79-100, Society of Material Science, Japan, 1981.

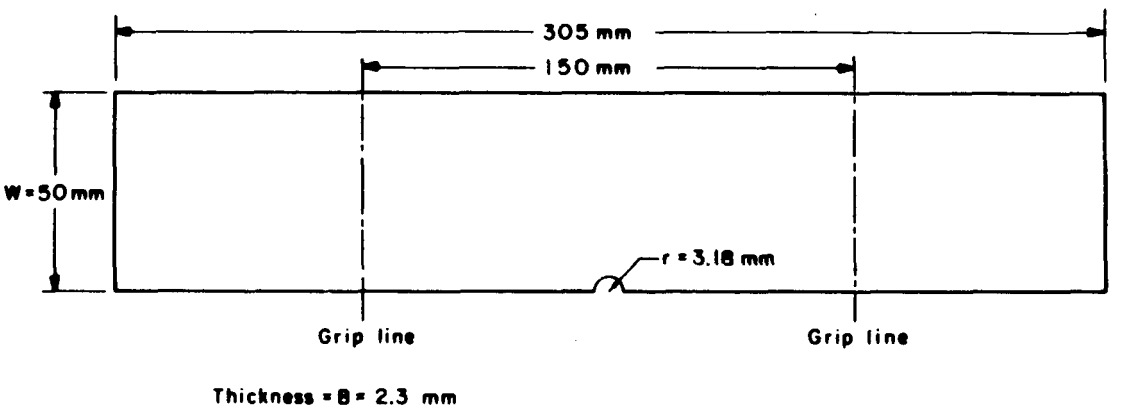

Figure 1. Dimension of the specimen with a single-edge notch.

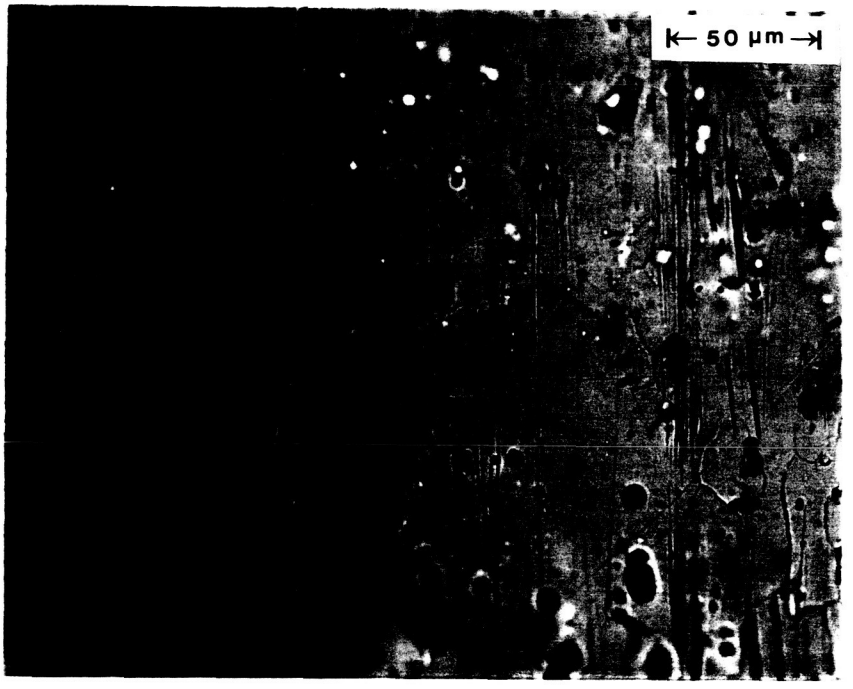

Figure 2. Indentations were placed with a spacing of 30 microns across a 100 micrometer long crack (400X)

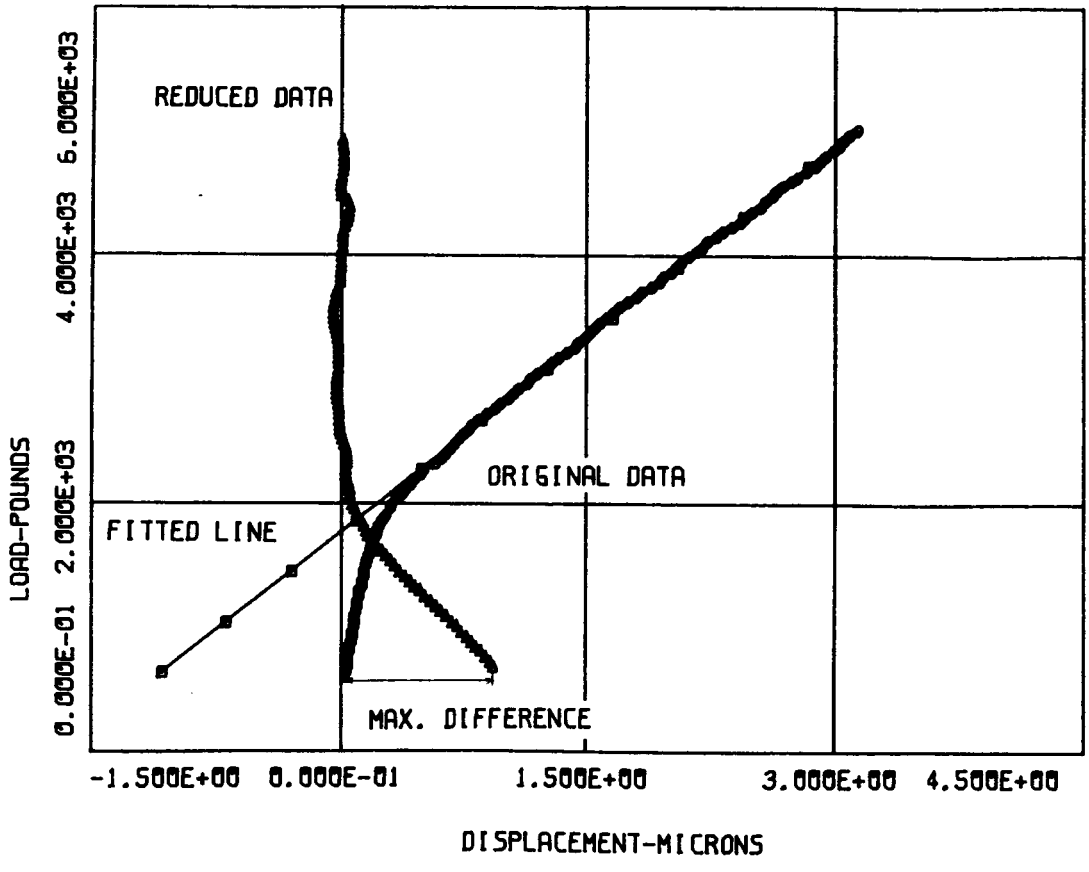

Figure 3. Reduced data method from a load-COD curve.

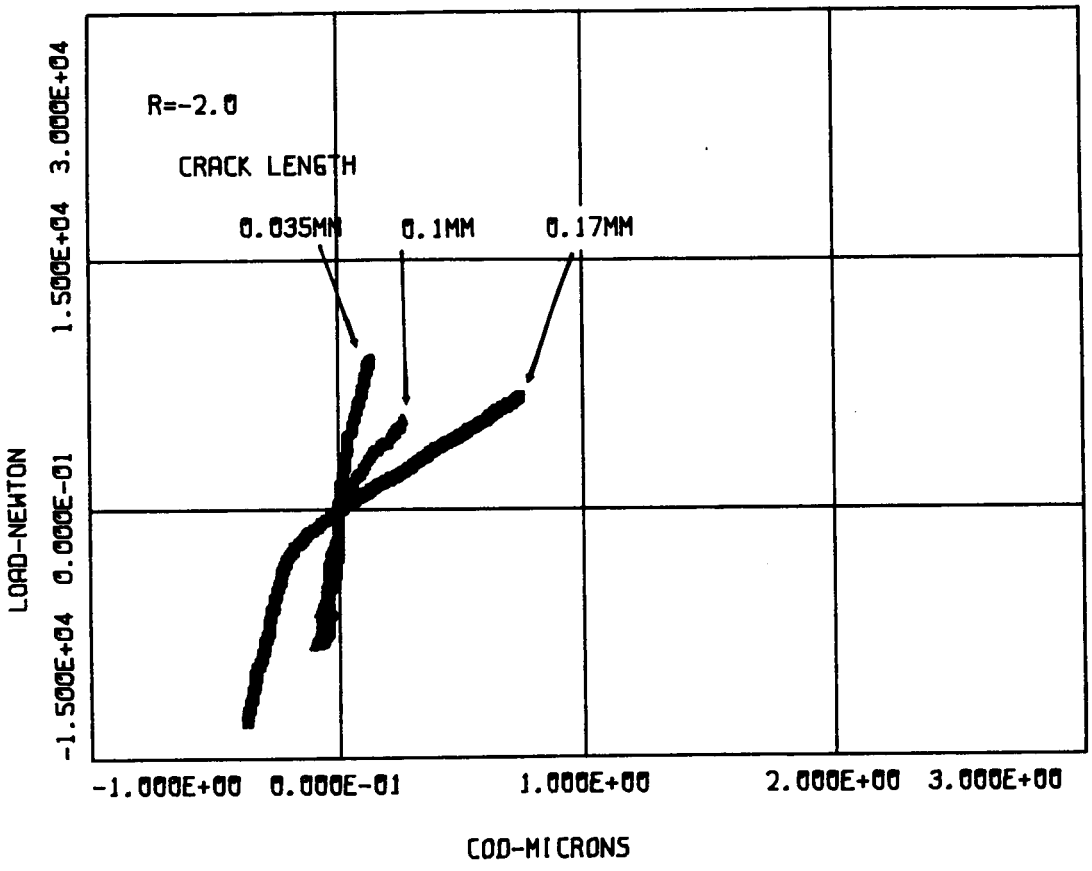

Figure 4. Typical load-COD plot for R = -2.

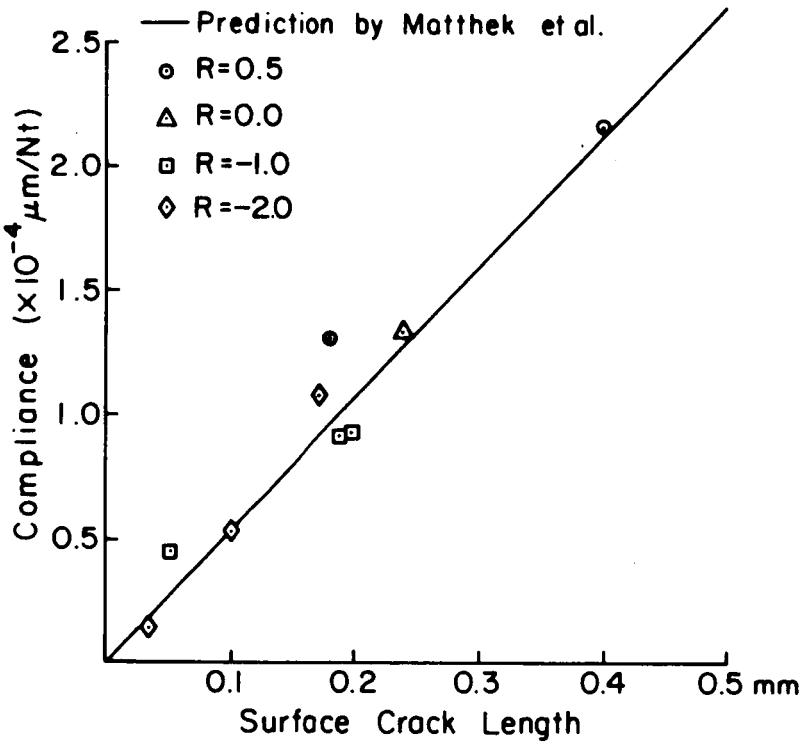

Figure 5. Plot of short crack compliances - surface crack length for semi-elliptical surface crack.

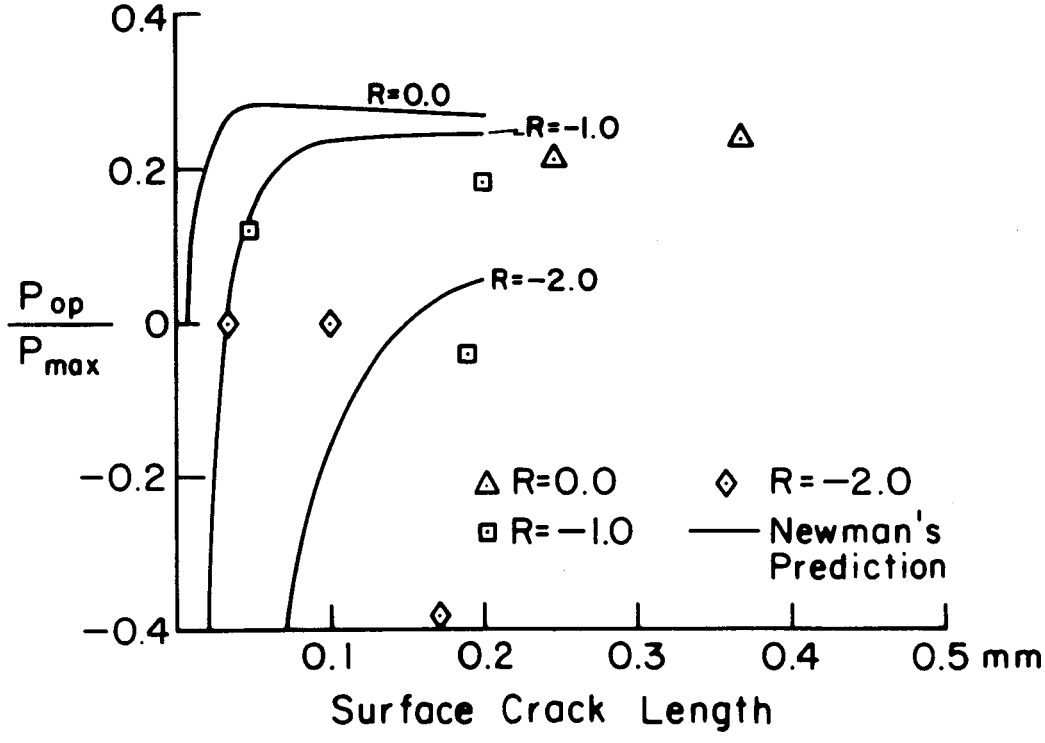

Figure 6. Plot of crack opening load-surface crack length for short surface cracks.

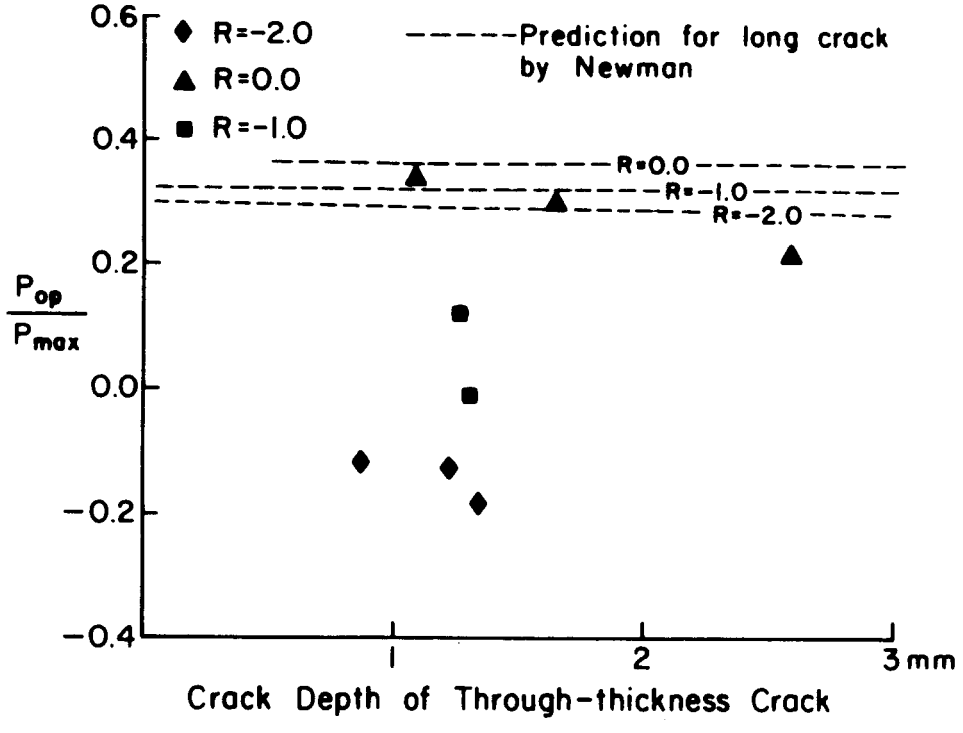

Figure 7. Plot of crack opening load ratio-crack length for through-thickness cracks.